Nickel nanoparticles supported on silica of low surface area. Hydrogen chemisorption and TPD and catalytic properties

Abdel-Ghani Boudjahem [a], Serge Monteverdi [a], Michel Mercy [a], Djaafar Ghanbaja [b] and Mohammed M. Bettahar [a,*]

[a] *Laboratoire de Catalyse Hétérogène, UMR CNRS 7565, Faculté des Sciences, Université Henri Poincaré, Nancy-I, BP 239, 54506 Vandœuvre Cédex, France*

[b] *Service Commun de Microscopie Electronique, Faculté des Sciences, Université Henri Poincaré, Nancy-I, BP 239, 54506 Vandœuvre Cédex, France*

Received 24 May 2002; accepted 15 August 2002

Nickel metal nanoparticles supported on silica of low surface area ($15\,m^2\,g^{-1}$) were prepared by reduction of nickel acetate by hydrazine in aqueous medium. Their gas-phase stability and surface properties depended on thermal pre-treatment under H_2 or air atmosphere. Small nickel particles (<10 nm), in oxidized or reduced state, are strongly resistant to reductive or oxidative treatment respectively. For H_2-treated catalysts, H_2 chemisorption and TPD results suggested the occurrence of spillover hydrogen between the metal nickel phase and silica. For air then H_2 treated catalysts, hydrogen spillover seemed to involve the NiO phase. The activity of the catalysts in gas-phase benzene hydrogenation also depended on the thermal pre-treatment. Pre-calcined then reduced catalysts exhibited higher TOFs than non pre-calcined catalysts, suggesting that the presence of NiO phase may have influenced the hydrogenation process.

KEY WORDS: supported nanonickel catalysts; hydrazine; hydrogen chemisorption and TPD; benzene hydrogenation.

1. Introduction

Conventional supported metal catalysts are prepared by *in situ* reduction of a metal salt. The catalytic activity of the metal particles formed is strongly related to their size and shape [1–6]. However, it is often difficult to control the morphology of the final material, notably for impregnated catalysts [7]. An alternative method to obtain supported catalysts with well-defined metal particles is the preparation of supported catalysts from metal colloids.

Metal nanoparticles research has recently become the focus of intense work due to their unusual properties as compared to the bulk metal [8,9]. They hold promise for use as advanced materials [10] and have also been applied in heterogeneous catalysis [7,10–15]. The chemical route of preparation of such materials is of specific interest since it allows a better structure control at the microscopic level [16–21]. The chemical methods have generally involved the reduction of the relevant metal salt in the presence of a stabilizer such as linear polymers [11,22,23], ligands [8,24], surfactants [22,25], tetraalkylammonium salts [26] or heterogeneous supports [27] which prevent the nanoparticles from agglomerating.

Previous work of our group showed that supported nickel nanoparticles can be obtained in an organic medium by reducing nickel acetate by NaH in the presence of an alcoholate surfactant [14,15]. They were found as active catalysts in gas-phase hydrogenation of 15. The stability and activity of the nanoparticles depended on the nature of the pre-treatment and nickel loading.

Recent works have pointed out the interest of working in water as a practical solution for the future in homogeneous and heterogeneous catalysis [28]. This prompted us to undertake a study of nickel nanoparticles obtained by reduction of nickel salts in aqueous medium and stabilized on a silica support of low surface area. The surface properties of the obtained catalysts were tested in the gas-phase hydrogenation of benzene.

Despite the great number of studies in the past decades, increasing attention is being paid to the hydrogenation of aromatics because of the stringent environmental regulations governing their concentration in diesel fuels [29,30]. Benzene hydrogenation has been chosen as the model aromatic feedstock [31–34]. This reaction has also been used as a model reaction in heterogeneous catalysis by metals where metal-support interactions are involved [32–35]. Hydrazine was used because recent studies showed it is a good reducing agent in aqueous medium of noble and transition metal ions [36,37]. As to the silica support, it is known to not give rise to nickel mixed oxides and allows a better approach of the particle size effect in the behavior of supported nickel catalysts. Moreover, generally speaking, nickel supported catalysts have been concerned with high surface area supports and nickel loading higher than 5 wt%. Also, the use of silica of low surface area and low nickel loading in the preparation of nickel-based catalysts was expected to give rise to an important contribution to the existing body of literature on Ni/SiO_2 systems [38].

* To whom correspondence should be addressed.

1011-372X/02/1100-0115/0

In the present study we report the results obtained for nickel nanoparticles (1–5 wt%) supported on silica of low area ($15\,m^2\,g^{-1}$) and obtained by reduction of nickel acetate by hydrazine in aqueous medium. The stability and surface properties of these particles were examined under hydrogen or air atmosphere and correlated to their catalytic activity in benzene hydrogenation. The catalysts were characterized by XRD, TEM and hydrogen chemisorption and TPD.

2. Experimental

2.1. Catalyst preparation

The silica support (Chempur, 99.99%) of $15\,m^2\,g^{-1}$ and grains of 325 mesh was pre-treated in air at 500 °C before use and stored under argon. It was impregnated at room temperature with 1.0–5.0% Ni wt using nickel acetate (≥99.0%, Fluka) as precursor, and after evaporating (80 °C) the aqueous solution the obtained solid was dried at 100 °C for 16 h.

The preparation of the supported nickel particles was performed under argon atmosphere. A suspension of the supported nickel precursor was stirred for 20 min at room temperature, then 10 ml of 24–26% aqueous hydrazine in excess (≥99.0%, Fluka) was added. The pH of the solution was 10–12 and remained almost constant during the reduction process. The reaction mixture was slowly heated from room temperature up to 80 °C and changed from translucid to dark color. After 30 min the black suspension was filtered, washed and dried at 60 °C under vacuum.

2.2. Catalyst characterization and testing

Nickel composition and specific area of the catalysts were determined on a Varian AA1275 atomic absorption spectrophotometer and Carlo Erba Sorptomatic 1900 equipment respectively. XRD patterns $I(\theta)$ and electron microscopy images were recorded at a classical $\theta/2\theta$ diffractometer using Cu K_α radiation and a Phillips CM20 STEM respectively.

Chemisorption and thermal treatment experiments were carried out with a sample of 100 mg on a pulse chromatographic microreactor, equipped with the catharometric detector of a microchromatograph (AT M200, Hewlett-Packard) fitted with molecular sieve columns and MTI software. Thermal treatment of the sample was conducted with a flow rate of $50\,ml\,min^{-1}$ and a heating temperature of $10\,°C\,min^{-1}$ up to 300–500 °C or 250 °C with pure H_2 or air respectively. For chemisorption studies the catalyst was further purged under argon flow for 2 h, cooled down to room temperature, then the reactant gas (100 ppm H_2/argon or 150 ppm O_2/helium respectively) was injected in the reactor every 2 min. The subsequent TPD of hydrogen was conducted after purging under argon flow for 2 h, then flowing with the same gas ($50\,ml\,min^{-1}$) in programmed temperature with a heating rate of $7.5\,°C\,min^{-1}$ up to 700 °C.

The gas-phase hydrogenation reaction was carried out in a quartz fixed-bed reactor at atmospheric pressure and in the temperature range 75–225 °C with a sample of 50 mg, a feed gas of 1% C_6H_6/H_2 and total rate flow of $50\,cm^3\,min^{-1}$. The reactant and product analysis were conducted on line using a Hewlett-Packard 5730A FID gas chromatograph equipped with TCEP (2 m, $\frac{1}{8}$ in.) and Sterling (3 m, $\frac{1}{8}$ in.) columns.

The utilized gases were purchased from Air Liquide. Oxygen traces were eliminated from argon (99.995%) and hydrogen (99.995%) by using a manganese oxytrap (Engelhardt), whereas helium (99.999%) and synthetic air were used as received. Oxygen diluted in argon was used as such.

3. Results and discussion

Our study showed that the degree of reduction and size of the nickel nanoparticles obtained depended on the concentration of the nickel salt or hydrazine, pH of the solution, temperature and time of reduction, presence or not of a stabilizer or support and metal loading. Typical results are presented below in the case of the 3% Ni/SiO_2 catalyst.

3.1. Characterization

3.1.1. XRD study

The spectrum of the fresh supported catalyst exhibited a main and large band at $2\theta = 44.5°$ characteristic of the metallic nickel phase of *cfc* structure. The particle size, as estimated using the Debye–Sherrer equation, was 12 nm. The spectrum also presented the signal of $Ni(OH)_2$ at $2\theta = 38.5°$ of *hcp* structure. This result is in good agreement with recent literature data showing that nickel sulfate precursor formed Ni^{2+} complex with hydrazine at room temperature, which decomposed in pure Ni° at pH > 10 and $T > 85\,°C$ or in a mixture of Ni° and $Ni(OH)_2$ at pH = 14 and $T = 90\,°C$ [37].

The fresh sample exhibited the characteristic band of metallic nickel after H_2/300 °C (figure 1), or air/250 °C then H_2/300 °C treatment. In the former case, the particle size, as estimated using the Debye–Sherrer equation, was 17 nm. Strikingly, the characteristic band of metallic nickel persisted when the fresh catalyst was treated solely in air/250 °C and any NiO signal was evidenced. Besides, in this case, the mean nickel particle size decreased down to 8 nm. The persistence of the Ni° band was ascribed to that part of the initial metallic nickel which resisted oxidation under air at 250 °C and probably consisted of small aggregates. These aggregates

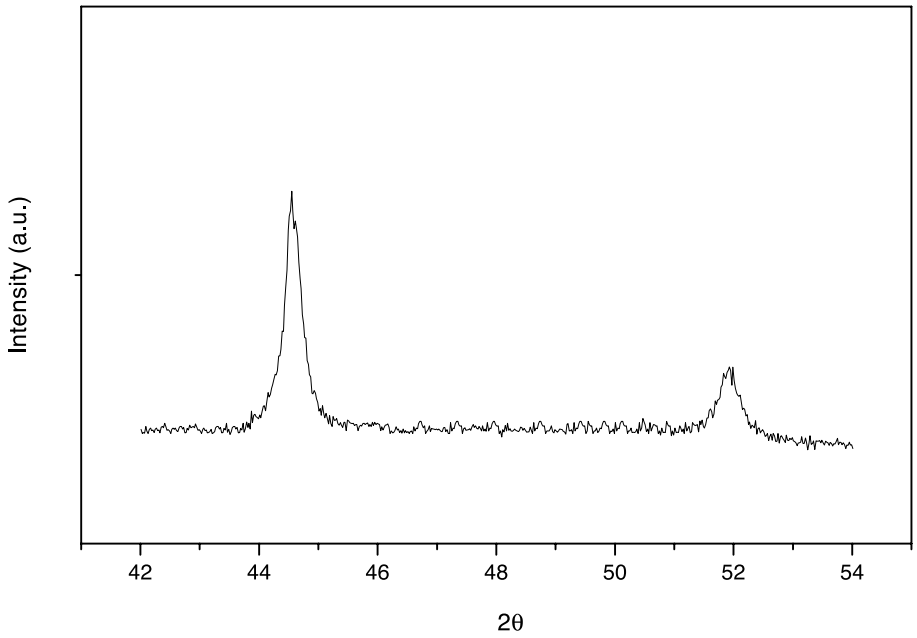

Figure 1. XRD spectrum of the non-calcined catalyst.

were not prone to oxidation, presumably because of the existence of chemical interaction with the support or low rate of nucleation during the oxidation process. As to the remaining metallic part, comprising larger particles, it was probably more easily oxidized in the NiO phase. The absence of a characteristic band for this phase suggests its high dispersion on the silica support; the oxide particles formed were probably attached to the support by strong Ni^{2+}–O bonds, and were thus less prone to sintering during the thermal oxidizing treatment.

3.1.2. TEM studies

The TEM experiments indicated that after hydrogen treatment at 300 °C the metal nanoparticles were relatively homogeneously dispersed on the support (figure 2). The average particle size was about 15 nm, in good agreement with the above XRD study. However, subnanoparticles are also present. In addition, a close inspection of the micrographs showed that the particles were of different geometrical shapes, among them triangular and hexagonal. HRTEM studies are necessary to obtain more information on the morphology of the present nickel catalyst.

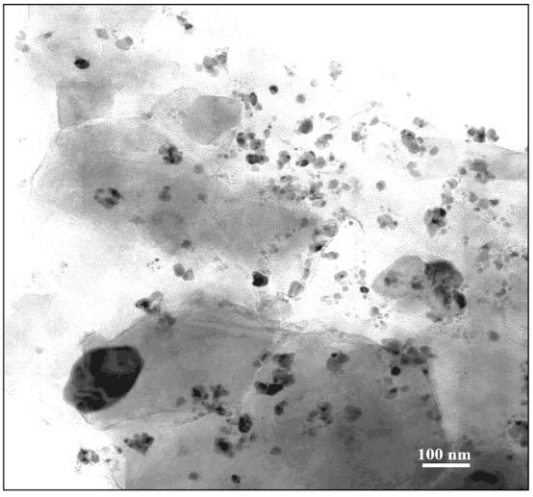

Figure 2. TEM of the non-calcined catalyst.

3.2. Chemisorption studies

3.2.1. Study of the support

The behavior of the silica support under hydrogen flow was studied. It was previously treated by aqueous hydrazine, then dried in the same conditions as the supported nickel catalysts. Adsorption and TPD of H_2 were performed after a previous treatment under H_2 at 400 °C.

The obtained results showed that silica did not adsorb hydrogen at all at room temperature. However, more strikingly, the TPD study showed that some hydrogen desorbed ($6.8\,\mu mol\,g_{supp}^{-1}$) from 300 °C (figure 3). The temperature profile consisted of a main peak at 598 °C with several shoulders at lower (431 °C, 502 °C) and higher (650 °C) temperatures. The desorbed gas was attributed to hydrogen retained in the silica support during the thermal hydrotreatment. Earlier works showed that silica dissolved H_2 at high temperature (around 1000 °C) as a result of the hydroxylation of silica by reduction of Si^{4+} into Si^{3+} ions [39]. Besides, the obtained material desorbed both water and hydrogen molecules, on heating at high temperature also, as a result of dehydroxylation reactions [39]. Both adsorption and desorption of hydrogen are diffusion controlled [39]. Dissolution of hydrogen in refractory support at relatively low temperature (<500 °C) was observed only

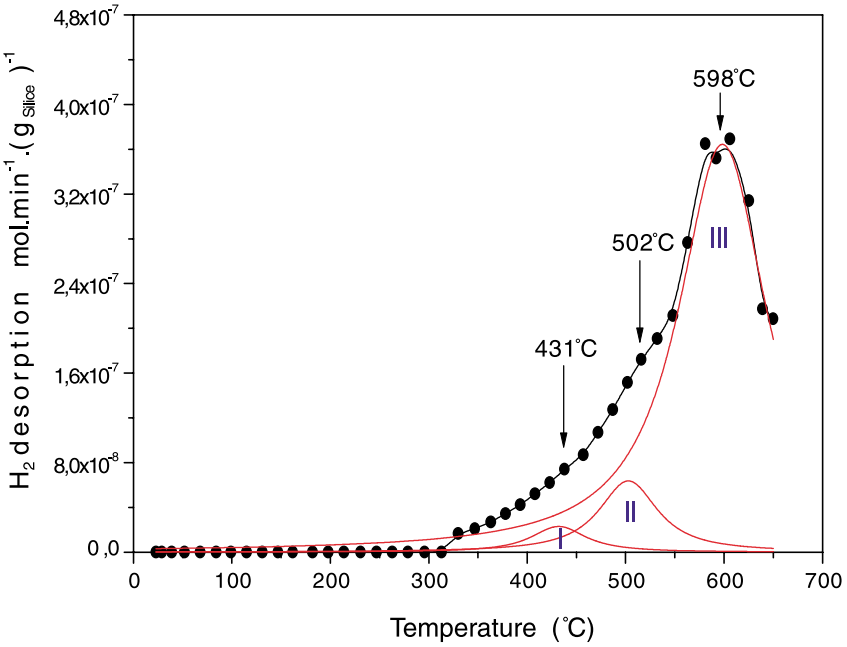

Figure 3. Hydrogen TPD of the bare support after treatment at 400 °C under H_2 flow.

in the presence of a metal phase and is known as spillover hydrogen [40,41]. In the present case, H_2 treatment at 400 °C may have activated silica defects, present in the precursor, or created new defects on which hydrogen molecules or atoms were strongly adsorbed.

3.2.2. Study of the non-calcined catalysts

The fresh catalysts almost did not chemisorb hydrogen and this was attributed to the presence of the organic acetate fragment, stemming from the nickel precursor salt, which inhibited the access of the H_2 molecules to the metal active phase [14,15]. Also, the study of adsorption at room temperature and TPD of H_2 was performed with catalysts treated under H_2 at 300, 400 or 500 °C for 1 or 2 h.

Classical supported nickel catalysts reduced by gaseous hydrogen give rise to H_2 TPD profiles comprising two or more peaks of temperature as a result of the formation of several active sites [41]. These catalysts, as other transition metal catalysts, are also good H_2 reservoirs, capable of large amounts of H_2 adsorption and storage [14,43,44]. The same behavior was observed for our nickel catalysts. The obtained results are reported in figure 4 and table 1.

The amount adsorbed passed through a maximum value for a temperature of pre-treatment of 400 °C (18.1 μmol g_{cat}^{-1}). The lower amount of hydrogen adsorbed was attributed to the presence of the acetate organic fragment not completely decomposed, or to sintering of the nickel phase when the temperature of pre-treatment was 300 or 500 °C respectively [14,15]. A pre-treatment temperature of 400 °C seemed to be a good compromise between the two opposite effects.

The TPD profiles (figure 4) showed that desorption of hydrogen comprised two domains of temperature. In the first domain two large peaks were observed at 80 °C and 185 °C respectively for the three samples. These peaks, denoted type I and I′ respectively, were ascribed to hydrogen weakly and strongly linked to nickel active sites respectively. The broad width of these peaks suggested the presence of small metal particles in good agreement with XRD and TEM experiments (see above). In the second domain a third peak (denoted type II) appeared at a temperature increasing (300, 550 or 650 °C) with the temperature of pre-treatment (300, 400 or 500 °C).

Table 1 shows that the amount of desorbed hydrogen increased with the temperature of hydrotreatment: from 11.3 μmol g_{cat}^{-1} to about 20.0 μmol g_{cat}^{-1} for 300 °C and 400–500 °C respectively. According to the TPD study of bare silica, part of this hydrogen may have arisen from the support. Besides, the increase in hydrogen storage was mainly due to the contribution of hydrogen of type II; this contribution was 70% for the treatment at 500 °C and 55% only for the treatment at 300 or 400 °C. Since the nickel phase seemed to collapse to a certain extent at 500 °C (table 1), an increase in storage capability would be ascribed to the intervention of the support, *i.e.*, spillover hydrogen [40,41]. It is worth noting that the bare support adsorbed and desorbed hydrogen at high temperatures (see above). We speculated that hydrogen transfer between nickel and silica, then hydrogen storage, was favored at high temperatures because support reactivity toward hydrogen and hydrogen diffusion rate in silica were increased.

The amount of hydrogen chemisorbed decreased a little with time of hydrotreatment, from 18.1 μmol g_{cat}^{-1}

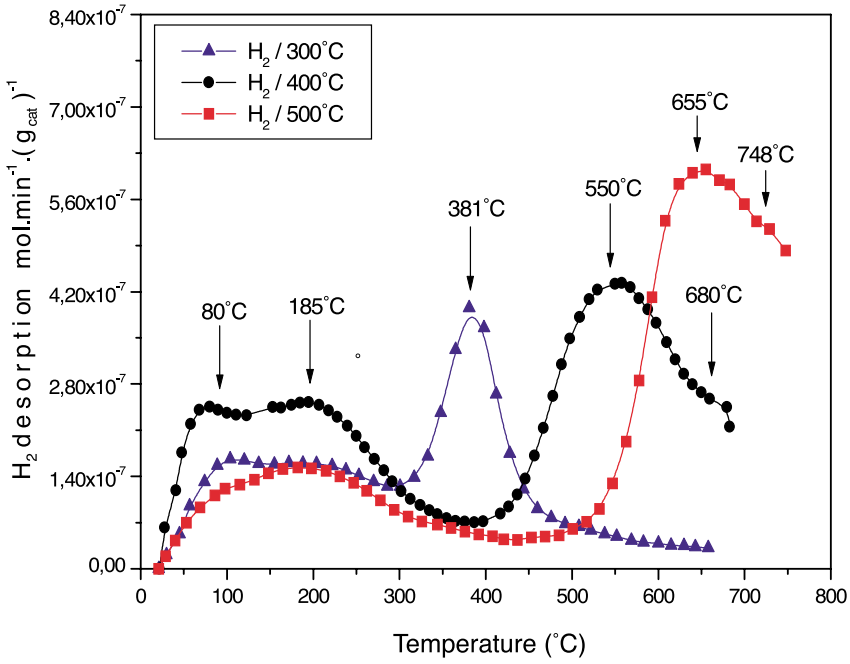

Figure 4. Effect of the temperature of the hydrotreatment on hydrogen TPD for the non-calcined nickel catalyst.

to 15.1 μmol g_{cat}^{-1} when the time of hydrotreatment was increased from 1 to 2 h (table 1). This was attributed to sintering of the nickel phase. In contrast, in the mean time, hydrogen desorption increased from 19.9 μmol g_{cat}^{-1} to 34.9 μmol g_{cat}^{-1} and the increase was mainly due to (70%) adsorption on sites of type II. Then, increasing the time of hydrotreatment also tended to both sinter the active phase and enhance hydrogen storage capability of the catalyst. These conclusions strengthen the assumption of the occurrence of spillover hydrogen for our nickel catalysts. Other works in hand confirm the phenomenon. For example, diluting the supported nickel particles in silica led to a higher amount of hydrogen stored.

3.2.3. Study of the calcined catalysts

Fresh catalyst samples were calcined at 250 °C, then reduced under hydrogen flow at 300 or 400 °C, and the effect of hydrothermal treatment on their surface was studied. The temperature profiles of both calcined and non-calcined catalysts were similar but differences appeared in the amounts of hydrogen. These differences were partly due to the presence of unreduced nickel particles. Also, the degree of reduction of the pre-calcined catalysts was determined by chemisorption of O_2 at 400 °C [45].

The degree of reduction increased from 79.5 to 87.8% when the temperature of treatment was increased from 300 to 400 °C, and from 63.4 to 87.8% when the time of treatment was increased from 1 to 2 h (table 2). These results show that the oxidized metal nanoparticles were resistant to reductive H_2 thermal treatment as reported for classical nickel catalysts in their oxidized state, irrespective of the type of support [2–6,46]. Such a behavior was accounted for by the existence of chemical interaction with the support.

Table 1
Chemisorption and TPD experiments on the Ni/SiO_2 catalysts. Effect of the thermal pre-treatment.

Pre-treatment		H_2 uptake (μmol g_{cat}^{-1})	H_2 desorption (μmol g_{cat}^{-1})		
			Total	At $T < T_H$ [a]	At $T > T_H$
Non-calcined	H_2/300 °C/1 h	9.4	11.3	5.1	6.2
	H_2/300 °C/2 h	7.5	14.4	4.0	10.4
	H_2/400 °C/1 h	18.1	19.9	8.9	11.0
	H_2/400 °C/2 h	15.1	34.9	10.5	14.4
	H_2/500 °C/1 h	7.4	19.3	5.9	13.4
Calcined [b]	H_2/300 °C/2 h	6.3	–	–	–
	H_2/400 °C/1 h	10.7	19.5	6.2	13.3
	H_2/400 °C/2 h	9.1	–	–	–

[a] T_H: temperature of hydrotreatment.
[b] Air/250 °C/2 h.

Table 2
Degree of reduction, turnover frequencies (TOF) and energy of activation for calcined and non-calcined catalysts.

Pre-treatment		Degree of reduction (%)	TOF molec. benz. s^{-1} $site^{-1}$		Ea ($kJ\,mol^{-1}$)
			75 °C	175 °C	
Non-calcined	H_2/300 °C/2 h	–	0.033	0.376	46.7
	H_2/400 °C/2 h	–	0.011	0.165	46.5
Calcined	H_2/300 °C/2 h	79.5	0.040	0.419	45.2
	H_2/400 °C/2 h	87.8	0.013	0.252	51.3
	H_2/400 °C/1 h	63.4	–	–	–

As a consequence of the presence of unreduced nickel, the calcined catalysts adsorbed less hydrogen than the non-calcined ones. In effect, after pre-treatment by H_2 at 400 °C for 1 or 2 h the calcined sample adsorbed 42.5 or 39.7% fewer respectively (table 1). A second important difference between calcined and non-calcined catalysts seemed to reside in their higher capability to store hydrogen. In effect, as shown in the case of the hydrotreatment at 400 °C/1 h (table 1), the calcined catalyst desorbed a higher amount (19.5 $\mu mol\,g_{cat}^{-1}$) than it adsorbed (10.4 $\mu mol\,g_{cat}^{-1}$). We may conclude that the presence of oxidized nickel particles enhanced the hydrogen reservoir of our catalysts. Besides, the hydrogen stored was mainly held on the strongest active sites (type II) of the catalyst surface: 70% of the total amount of hydrogen desorbed, against 55% for the non-calcined catalyst (table 1). Then, as far as spillover hydrogen was concerned (see above), the NiO particles were probably involved in the internal transfer of atomic or molecular hydrogen. The previous oxidizing treatment may have induced specific Ni–Al interactions which favored hydrogen storage [43].

3.3. Catalytic activity

In the absence of thermal pre-treatment the supported nanoparticles were inactive in the gas-phase hydrogenation of benzene in cyclohexane. After thermal treatment the catalysts became active and selective. Only traces of cyclohexane and methylcyclopentane were detected. The catalysts exhibited a maximum of conversion as a function of the reaction temperature. This maximum was reached around 175 °C at a conversion of 95–100% for all catalysts and was attributed to the competitive adsorption between benzene and H_2 reactant molecules [15,31]. The bare silica support, previously treated in aqueous hydrazine, was found to be inactive.

3.3.1. Effect of the temperature and duration of H_2 pre-treatment for the non-calcined catalysts

The effect of the H_2 pre-treatment on the activity of the catalysts was studied in the temperature range 200–400 °C for a duration of 2 h. The best activity was obtained at a temperature of hydrotreatment of 300 °C (figure 5). The lower activity observed at the pre-treatment temperatures of 200 or 350 °C (400 °C) was ascribed to the presence of the incompletely decomposed organic matrix of the acetate precursor or sintering of nickel particles [14] respectively. We concluded that, in good accordance with the above chemisorption study (table 1), a pre-treatment temperature of 300 °C was probably a good compromise between two opposite effects: the organic matrix removal on one hand and the sintering of the metal particles on the other hand.

The effect of the pre-treatment at 300 °C on the catalyst activity was also studied for 1h, 2 h or 3 h. At the maximum of conversion (reaction temperature of 175 °C) the specific activities were 10.5, 12.3 and 11.5 $mol\,min^{-1}\,g_{Ni}^{-1} \times 10^{-3}$ respectively. The best time of hydrotreatment of 2 h was ascribed to the compromise between organic matrix removal and metal particle sintering.

We calculated the turnover frequencies (TOF) for the reaction temperatures of 75 and 175 °C (table 2). The results at 75 °C (0.012–0.033) are in good agreement with that recently reported for classical Ni/SiO_2 catalysts at 80 °C (0.005–0.025) [38]. On the other hand, TOF increased, whereas the accessible surface area decreased. When the hydrotreatment temperature was increased from 300 to 400 °C for 2 h, TOF was multiplied by 2.3–3.0, whereas a chemisorbed hydrogen amount was divided by 2.0. Recent discussions on gas-phase hydrogenation of benzene on nickel catalysts concluded that it was a structure-sensitive reaction, but generalization may be risky [34,38]. Nevertheless, it is generally accepted that reactions are structure sensitive for gaps in TOF much higher than 3 and metal particle size below 3–5 nm [32–35,38]. In the present case the gap in TOF is below ($\leq$3) and metal particle size above (around 10 nm) these values for structure-sensitive reactions [32–35,38]; benzene hydrogenation appeared as structure-insensitive reaction in our conditions.

The energy of activation was about 47.0 $kJ\,mol^{-1}$ in the temperature range 75–150 °C and did not depend on the temperature of pre-treatment. The obtained value is in good agreement with that reported in the literature for classical nickel catalysts (50.0–58.0 $kJ\,mol^{-1}$) [32,34].

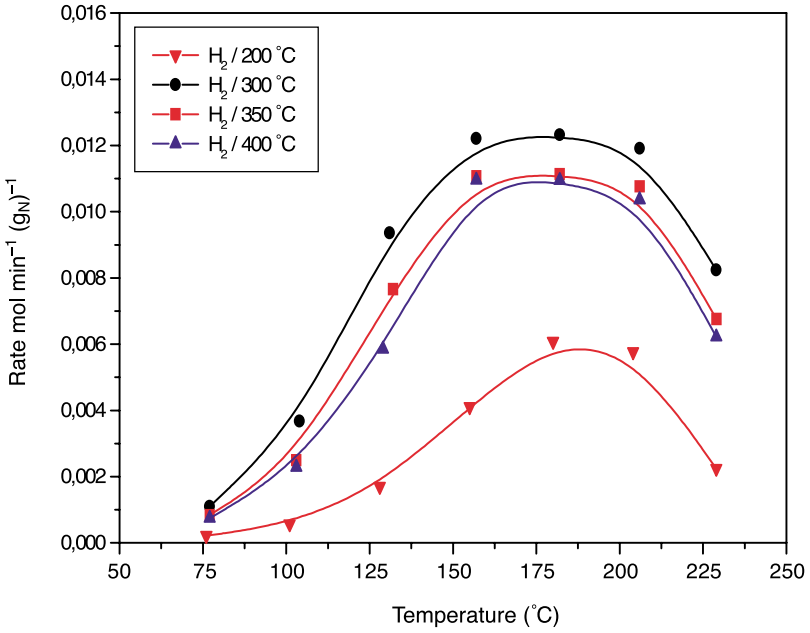

Figure 5. Effect of the hydrotreatment temperature on the catalytic activity for the non-calcined nickel catalyst.

3.3.2. *Effect of the temperature of H_2 pre-treatment for the calcined catalysts*

The effect of previous oxidizing pre-treatment on the catalytic properties of the nickel nanoparticles was examined. For this purpose the fresh supported nanoparticles were first calcined at 250 °C, then reduced under hydrogen at 300 or 400 °C for 2 h. As for the non-calcined catalysts the activity was diminished when the hydrotreatment temperature was increased; the decrease was 15–33% and this difference accounted for the occurrence of sintering of the nickel phase (table 2). The activity also seemed not to be correlated to the metal surface area (table 2); TOF was multiplied by 1.7–3.0 when that of chemisorbed hydrogen was divided by 1.4. Besides, the calcined catalysts appeared as more active than the non-calcined catalysts; for the same temperature of hydrotreatment (300 or 400 °C) the TOF was higher (11–17 or 15–35%) (table 2). Such a change in the behavior of the nickel nanoparticles may be related to the presence of unreduced nickel in the calcined catalysts, as suggested by other authors [34,47,48]. These authors believe that unreduced nickel decreased the size of the nickel particles required for the adsorption of benzene in planar mode [34,48].

The energy of activation was 45.2 or 51.3 kJ mol^{-1} in the temperature range 75–150 °C when the temperature of hydro pre-treatment was 300 or 400 °C respectively. These values are in good agreement with those observed for the above non-calcined catalysts. The similar energy of activation for both types of catalyst indicates that the presence of unreduced nickel did not change the reaction mechanism of gas-phase hydrogenation of benzene.

4. Conclusions

We have studied the stability and surface properties of nickel metallic nanoparticles obtained by reduction of nickel acetate by hydrazine in aqueous medium and supported over silica of low surface area. The XRD, TEM and hydrogen adsorption studies showed that the mean size of fresh particles increased under H_2 flow; all the more the temperature and time of hydrotreatment increased (from 12 nm up to 17 nm at 300 °C/2 h). The smallest metal particles were resistant to oxidative thermal treatment which, besides, decreased their mean size (down to 8 nm under air/250 °C). Conversely, previously calcined particles under air/250 °C were resistant to reduction under H_2 flow at 300–500 °C.

The TPD profiles of hydrogen exhibited two domains of temperature. The first domain consisted of two peaks of temperature at 90 and 200 °C ascribed to hydrogen weakly and strongly linked to nickel active sites respectively. This domain was not pre-treatment temperature dependent. In the second domain a large peak appeared at a temperature (400–650 °C) and with a surface area increasing with the temperature and time of pre-treatment. This peak was ascribed to hydrogen, much more bounded to the catalyst surface. The bare support also desorbed non-negligible amounts of hydrogen at high temperature (>500 °C). The whole TPD results strongly suggested the occurrence of spillover hydrogen from the nickel phase onto the silica support. Unreduced nickel also seemed to be involved in hydrogen spillover in the case of the pre-calcined catalysts.

The supported nickel nanoparticles exhibited high activity in benzene hydrogenation, provided the organic fragment of the metal precursor was decomposed under

hydrogen or air at moderate temperature. High temperature and a longer time of hydrotreatment depressed the catalyst efficiency as a result of the nickel phase sintering. Strikingly, the activity of the calcined catalyst was found to be higher than that of the non-calcined catalyst and was correlated to the presence of unreduced nickel phase.

References

[1] T.S. Armadi, Z.L. Wang, T.C. Green, A. Heinglein and M.A. El-Sayed, Science 272 (1996) 1924.
[2] S.J. Tautster and S.C. Fung, J. Catal. 5 (1978) 29.
[3] C.H. Bartholomew, R.B. Pannell and R.W. Fowler, J. Catal. 79 (1983) 34.
[4] J. Zelinski, J. Catal. 76 (1982) 157.
[5] J.T. Richardson, M. Lei, B. Turk, K. Forster and M.V. Twigg, Appl. Cat. 110 (1994) 217.
[6] R. Molina and G. Poncelet, J. Catal. 173 (1998) 257.
[7] A. Miyazaki, I. Balin, K. Aika and Y. Nakano, J. Catal. 204 (2001) 364.
[8] G. Schmid, Chem. Rev. 92 (1992) 1709.
[9] L.N. Lewis, Chem. Rev. 93 (1993) 2693.
[10] R.L. Whetten, Acc. Chem. Res. 32 (1999) 397.
[11] B.C. Gates, Chem. Rev. 95 (1995) 511.
[12] U.A. Paulus, U. Endrushchat, G.J. Feldmeyer, T.J. Schmidt, H. Bonnemann and R.J. Behm, J. Catal. 195 (2000) 383.
[13] E.A. Sales, B. Benhamida, V. Caizergues, J.P. Lagier, F. Fievet and F. Bozon-Verduraz, Appl. Catal. 172 (1998) 273.
[14] D. Franquin, S. Monteverdi, S. Molina, M.M. Bettahar and Y. Fort, J. Mater. Sci. 34 (1999) 1.
[15] S. Lefondeur, S. Monteverdi, S. Molina, M.M. Bettahar and Y. Fort, J. Mater. Sci. 36 (2001) 2633.
[16] J.H. Fendler and F.C. Meldrum, Adv. Mater. 7 (1991) 607.
[17] F. Fievet, F. Fievet-Vincent, J.P. Lagier, B. Dumont and M. Filgarz, J. Mater. Chem. 3 (1993) 627.
[18] R.D. Rieke, Acc. Chem. Res. 10 (1997) 377.
[19] G.A. Ozin, Adv. Mater. 4 (1992) 612.
[20] G.N. Glavee, Inorg. Chem. 32 (1993) 474.
[21] H. Bonnemann, W. Brijoux and T. Joussen, Angew. Chem. (Int. Ed. Engl.) 29 (1990) 273.
[22] N. Toshima and Y. Wang, Adv. Mater. 6 (1994) 245.
[23] J.S. Bradley, J.M. Millar, E.W. Hill, S. Behal and B. Chaudret, Faraday Discuss. 92 (1991) 255.
[24] C. Amiens, D. de Caro, B. Chaudret, J.S. Bradley, R. Mazel and C. Roucau, J. Amer. Chem. Soc. 115 (1993) 11638.
[25] K. Esumi, K. Matzuhita and K. Torigoe, Langmuir 11 (1995) 3285.
[26] M.T. Reetz and W. Helbig, J. Amer. Chem. Soc. 116 (1994) 7401.
[27] R. Brayner, G. Viau, G.M. da Cruz, F. Fiévet-Vincent, F. Fiévet and F. Bozon-Verduraz, Catal. Today 57 (2000) 187.
[28] J.L. Pellegatta, C. Blandy, V. Collière, R. Choukroun, B. Chaudret, P. Cheng and K. Phillipot, J. Mol. Cat. A 178 (2002) 55.
[29] A. Stanislaus and B.H. Cooper, Catal. Rev. Sci. Eng. 36 (1994) 75.
[30] K. Weissermel and H.J. Arple, in: *Industrial Organic Chemistry*, 3rd Ed. (VCH, New York, 1997).
[31] M.A. Keane, J. Catal. 166 (1997) 347.
[32] K.J. Yoon and M.A. Vannice, J. Catal. 82 (1983) 457.
[33] L. Daza, B. Pawelec, J.A. Anderson and J.L.G. Fierro, Appl. Catal. 87 (1992) 145.
[34] R. Molina and G. Poncelet, J. Catal. 199 (2001) 162.
[35] R. Burch and R. Flambard, J. Catal. 85 (1984) 16.
[36] A. Bensalem, G. Shafeev and F. Bozon-Verduraz, Catal. Lett. 18 (1993) 165.
[37] Y.D. Li, L.Q. Li, H.W. Liao and H.R. Wang, J. Mater. Chem. 9 (1999) 2675.
[38] R. Takahashi, S. Sato, T. Sodesawa, M. Kato, S. Takenaka and S. Yoshida, J. Catal. 204 (2001) 259.
[39] P. Pascal, in: *Nouveau Traité de Chimie Minerale*, Masson Ed., Vol. VIII, 1965, p. 93.
[40] S.T. Srinivas and P. Kanta Rao, J. Catal. 148 (1994) 470.
[41] J.L. Carter, in: *Proceedings, 3rd International Congress on Catalysis, Amsterdam, 1964* (Wiley, New York, 1965) p. 1.
[42] J.J.F. Sholten, A.P. Pijpers and A.M.L. Hustings, Catal. Rev. Sci. Eng. 27 (1985) 151.
[43] M.P. Sohier, G. Wröbel, J.P. Bonnelle and J.P. Marq, Appl. Catal. A 84 (1992) 169.
[44] D. Duprez, J. Barbier, Z. Ferhat-Hamida and M.M. Bettahar, Appl. Catal. 12 (1984) 219.
[45] C.H. Bartholomew and R.J. Farrauto, J. Catal. 45 (1976) 41.
[46] M. Houalla, F. Delannay and B. Delmon, J. Chem. Soc. Faraday Trans. 76 (1980) 2128.
[47] J.A. Anderson, L. Daza, J.L. Fierro and T. Rodrigo, J. Chem. Soc. Faraday Trans. 89 (1993) 3651.
[48] J.A. Anderson, L. Daza, S. Damayanova, J.L. Fierro and T. Rodrigo, Appl. Catal. 113 (1994) 75.